

# INTERNATIONAL JOURNAL OF MECHANICAL ENGINEERING AND TECHNOLOGY (IJMET)

ISSN 0976 – 6340 (Print)

ISSN 0976 – 6359 (Online)

Volume 4, Issue 2, March - April (2013), pp. 86-99

© IAEME: [www.iaeme.com/ijmet.asp](http://www.iaeme.com/ijmet.asp)

Journal Impact Factor (2013): 5.7731 (Calculated by GISI)

[www.jifactor.com](http://www.jifactor.com)



.....

## Ni ION RELEASE OF TiO<sub>2</sub> AND TiO<sub>2</sub>/ HYDROXYLAPATITE COMPOSITE COATINGS FORMED ON NiTi SHAPE MEMORY ALLOY PRODUCED BY POWDER METALLURGY

Sami Abualnoun Ajeel<sup>1</sup>, Abdul Raheem. K. Abid Ali<sup>2</sup>, Murtadha Abdulmueen Alher<sup>3</sup>

<sup>1</sup> Assist. Prof., Production Engineering and Metallurgy Department, University of  
Technology, Baghdad-Iraq

<sup>2</sup> Assist Prof., Materials Engineering College, University of Babylon,  
Babylon-Iraq

<sup>3</sup> Assistant Lecturer, Mechanical Engineering Department, University of Karbala,  
Karbala-Iraq

### ABSTRACT

Titania (TiO<sub>2</sub>) and TiO<sub>2</sub>/hydroxylapatite composite coatings (TiO<sub>2</sub>/HA) were formed on porous NiTi shape memory alloy using a H<sub>2</sub>O<sub>2</sub>-oxidation for TiO<sub>2</sub> coating and H<sub>2</sub>O<sub>2</sub>-oxidation+ KOH treatment technique and the subsequent accelerated biomimetic process for composite TiO<sub>2</sub>/HA coatings. Porous NiTi shape memory alloys prepared by powder metallurgy method. The powders were compacted at four different compacting pressures ( 200-800) MPa , then samples were sintered and heat treated. The XRD patterns for bare samples showed that the austenitic phase B2 and martensitic phase B19' and small amount of Ni<sub>3</sub>Ti phase, where the B2 and B19' are responsible of the shape memory effect for NiTi shape memory alloys. The XRD patterns for samples treated with H<sub>2</sub>O<sub>2</sub> showed the formation of crystalline TiO<sub>2</sub> in both forms (rutile and anatase). The XRD patterns of samples immersed in higher strength simulated body fluid 5SBF after treated with H<sub>2</sub>O<sub>2</sub> and KOH solutions, showed the formation of hydroxylapatite in addition to anatase and rutile. In the current investigation, Ni ion release testing in 0.9% NaCl solution at 37°C was employed to assess biocompatibility properties of TiO<sub>2</sub>/HA composite coatings formed on porous equiatomic NiTi SMA. The results showed that the Ni ion release increased with increasing the impression time and porosity. It has been also showed that single coat of TiO<sub>2</sub> is insufficient to reduce the Ni ion release below the safety line, while the composite coatings of TiO<sub>2</sub>/HA curves intersected the safety line and some of the points are lower than the safety line.

**KeyWords:** Porous, Powder Metallurgy, Shape Memory Alloys, Ni Ion Release, Hydroxylapatite, Titania, NiTi, Coating.

## **INTRODUCTION**

Equiatomic NiTi alloys have attracted much attention due to their shape memory effect, superelastic behavior, high tensile strength, good corrosion resistance and biocompatibility. These characteristics make NiTi alloys attractive for many biomedical applications, such as orthopedics applications, orthodontic applications, neurosurgical applications and catheterization applications [1,2].

In recent decades, porous NiTi shape memory alloys (SMAs) have drawn a great deal of attention as one of the promising biomaterials for orthopedic implants and hard-tissue replacements because of the combined virtue of the shape memory effect, superelasticity and adjustable mechanical properties, in particular the tailored pore structure of promoting tissue in-growth [3]. NiTi shape memory alloys typically is covered by a naturally formed thin adherent oxide layer of TiO<sub>2</sub> known as a passive film. This film is very stable and NiTi alloys are resistant to many forms of corrosive attack; however, this passive film is attacked by acidic solutions containing chloride [4]. In addition, the oxides formed on the Nitinol surface always contain a certain fraction of Ni. Contrary to pure titanium and Ti4Al6V medical alloys, which easily repassivate after surface damage, the Nitinol oxides have a lower self-healing ability in scratch tests, a lower resistance to localized corrosion [5]. Titanium dioxide TiO<sub>2</sub> coatings have been long considered as biocompatible interfaces to promote the physicochemical bonding between the bone tissues and implant material [6].

Hydroxylapatite(HA) also has been available clinically for use in dentistry and medicine in recent years due to its excellent biocompatibility and osteoconduction. The HA coating can satisfy the dual properties. HA is a major inorganic component of natural bone and can accelerate the bone growth. But the mechanical strength of HA is too poor to be used in load-bearing applications. In other hand metallic materials commonly exhibit poor bone bioactivity and good mechanical properties. To overcome this shortcoming, different methods to deposit a hydroxylapatite (HA) on metallic implants have been reported, including plasma spraying, pulsed laser deposition, sputter deposition, electrochemical deposition, electrophoretic deposition, sol-gel coating, biomimetic coating, etc [7]. It showed that the simulated body fluid (SBF) has almost the same ion concentrations as those of the human blood plasma and can well reproduce in vivo surface changes. Thus, it is a more efficient method to immerse the biomaterials into SBF for the investigation of the biological behavior of biomimetic deposition of apatite layer [8]. In many studies on HA coating and bioactive treatment, the substrates were titanium and its alloys. On the other hand, similar studies on NiTi SMAs are much less commonly reported, because of the shorter history of NiTi SMAs in implant applications compared with titanium. It is the objective of this study to investigate the effect of biocoatings on the Ni ion release of porous equiatomic NiTi shape memory alloy in 0.9% NaCl solution at 37 °C.

## **EXPERIMENTAL PROCEDURES**

Pure nickel and titanium powders were supplied by Merck Company. The powder elements mixing with equiatomic percentage of Ni and Ti for 5 hours with little amount of acetone and different sizes of alumina balls in the electrical mixer. The powders then

compacted by hydraulic press, for 200, 400, 600 and 800MParespectively in the cylindrical with the inner diameter 14 mm . Then green compacted samples sintered in the tube furnace attached with tube of quartz and protected atmosphere by argon gas. The sintering temperature was  $975 \text{ }^\circ\text{C} \pm 5 \text{ }^\circ\text{C}$  for 6 hours and the protected gas is continued during cooling until the samples reached to the room temperature. Heat treated for samples was achieved by heating the samples to  $900 \text{ }^\circ\text{C}$  in the tube furnace with flowing the protected atmosphere of argon for one hour then quenched in saline solution. All samples after sintering and heat treatment have been wet grinding using 180, 400, 800,1000,1200 and 2000 grit silicon carbide papers. Then samples polished with fine alumina type  $0.03 \text{ }\mu\text{m}$  fine polishing alumina. The green porosity is measured according to the general rule of density (weight/volume) and calculated the theoretical density of NiTi shape memory alloy from the density of each nickel and titanium elements according to equation below:

$$\rho_{tB} = \sum_{i=1}^n Wt_i * \rho_1 + Wt_2 * \rho_2 + Wt_3 * \rho_3 + \dots + Wt_n * \rho_n \quad (1)$$

$\rho_{tB}$  = theoretical density of blended powder ( $\text{g}/\text{cm}^3$ ).

$n$  = No. of elemental powders.

$W_i$  = weight percent (%).

$\rho_{1,2,3,\dots,n}$  = density of elemental powder ( $\text{g}/\text{cm}^3$ ).

The porosity for samples after sintering is measured according to ASTM B328 [9]. The phases formed after sintering and heat treatment detected using  $\theta$ -  $2\theta$  X-ray diffraction methods. X-Ray generator with Cu  $K\alpha$  radiation at 40 KV and 30 mA is used. The X-ray is generated by general electric diffraction type Philips (Pw 1840).The data were collected in  $2\theta$  range  $10$ - $80$  with a step size  $0.5^\circ$ .The target used in the x-ray tube was Cu, therefore  $\lambda_{\text{cu}} = 1.542 \text{ }^\circ\text{A}$  was used in obtaining the XRD patterns.

Samples divided into three groups. Group A stayed without coating. Group B and C are cleaned with acetone (10 min), ethanol (10 min) and distilled water rinsing (10 min) respectively. The samples are then boiled for 120 min in 35% aqueous  $\text{H}_2\text{O}_2$  and rinsed again with distilled water. Group B is stayed at this treatment and group C is etched with 4M aqueous KOH for 30 min at  $120^\circ\text{C}$ , followed by multiple rinse with distilled water. After this etching step for group C, the samples are immersed at  $37^\circ\text{C}$  in higher strength simulated body fluid (SBF), which is contain the 5 times contents of simulated body fluid as shown in Table.1, for 14 days.

The phases formed after coatings id detected by grazing incidence on a Philips X'pert diffractometer with  $\text{CuK}\alpha$  radiation, 40 kV, 30 mA, grazing incidence at  $5^\circ$ . The data were collected in the  $2\theta$  range  $10$ - $80^\circ$  with step size of  $0.0394^\circ$ .

After coating there are three groups of samples group A is a bare samples, group B samples that coated with  $\text{TiO}_2$  and group C samples coated with composite coating  $\text{TiO}_2/\text{HA}$ .

The release of nickel ion from the all groups of samples A,B and C are carried out in 0.9% NaCl saline solution. The samples are completely immersed into the 0.9% NaCl saline solution for seven weeks at  $37 \text{ }^\circ\text{C}$  in a water bath. The samples putted in the glasses containers with 40 ml of 0.9 % NaCl saline solution. The solution is not stirred. 5 ml of the solution is removed each week and used to determine the nickel concentration. This volume is not replaced to avoid contamination. The Ni ion release is measured by atomic absorption spectroscopy AAS.

The amount of released nickel per sample surface area (accumulated mass of released nickel,  $\mu\text{g}/\text{cm}^2$ ) is computed as:

$$M_{\text{Ni}} = V_1 \cdot C_{\text{Ni}} / S_{\text{surface}} \quad (2)$$

$V_1$  is the total solution volume (starting with 40 ml, then 35 ml, 30 ml, etc.),  $C_{\text{Ni}}$  the concentration of nickel in ppb( $\mu\text{g L}^{-1}$ ),  $S_{\text{surface}}$  the sample surface area and  $M_{\text{Ni}}$  the cumulated nickel release rate ( $\mu\text{g cm}^{-2}$ ).

<b>Component Constituent</b>	<b>Concentration g/l</b>
<b>NaCl</b>	<b>8.035</b>
<b>NaHCO<sub>3</sub></b>	<b>0.355</b>
<b>KCl</b>	<b>0.225</b>
<b>K<sub>2</sub>HPO<sub>4</sub>.3H<sub>2</sub>O</b>	<b>0.231</b>
<b>MgCl.6H<sub>2</sub>O</b>	<b>0.311</b>
<b>CaCl<sub>2</sub></b>	<b>0.292</b>
<b>Na<sub>2</sub>SO<sub>4</sub></b>	<b>0.072</b>

**Table 4.1**The composition of Simulated Body Fluid (SBF) [10].

## RESULTS AND DISCUSSION

The theoretical density measured from equation (1) is  $6.9 \text{ g/cm}^3$ . Green porosity calculated according to equation (3). Fig.1 shows the change of green porosity with compacting pressure. It is found that porosities are decreased after sintering, this reduction is attributed to the high temperature during sintering which led to reduce the size of pores in the structure and is rejected the air from the pores which move far from the samples by the flowing of argon during sintering. Fig.2 shows the change of porosity after sintering with compacting pressure.

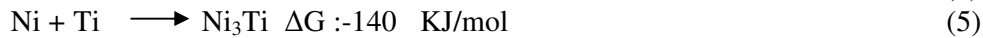
$$P_g = \left( 1 - \frac{\rho_g}{\rho_{IB}} \right) \times 100\% \quad (3)$$

$P_g$  = green porosity (%)

$\rho_g$  = green density ( $\text{g}/\text{cm}^3$ ).

$\rho_{IB}$  = theoretical density of blended mixture ( $\text{g}/\text{cm}^3$ ).

Fig.3 shows the XRD pattern for samples before sintering. It is clear that there are not any phases rather than pure Ni and Ti are formed before sintering. Fig.4 shows the XRD pattern after sintering. Fig.4 shows that all pure Ni and pure Ti transferred to NiTi phases and Ni<sub>3</sub>Ti phase, which proves that the sintering time and temperature that used in this work is resulted in complete sintering reaction. Fig.8 shows XRD pattern after heat treatment. Fig.5 shows that heat treatment led to increase the intensities of NiTi phases (NiTi monoclinic B19 phase which known as martensitic phase and NiTi cubic B2 phase which known as austenitic phase) and decrease the intensities of Ni<sub>3</sub>Ti. B2 and B19 phases, which are responsible of the shape effect in NiTi shape memory alloys. The formation of Ni<sub>3</sub>Ti might be attributed to the slow cooling of samples with the furnace [11]. The suggested reactions during the process are as follows [12]:



According to the binary phase diagram of Ni-Ti system [13], NiTi, Ni<sub>3</sub>Ti are stable compounds and reaction (5) is more thermodynamically favored than reaction (2),consequently, it is difficult to completely remove Ni<sub>3</sub>Ti from sintered sample [12].

XRD pattern in Fig.6 indicates that the main phases present when NiTi samples treated with H<sub>2</sub>O<sub>2</sub> for two hours are TiO<sub>2</sub> in both anatase, rutile forms, NiTi (B2, B19') phase and Ni<sub>3</sub>Ti. No nickel oxide is detected. This is due to the fact that the free energy for the formation of nickel oxide is much higher than that of the titanium oxide ( $\Delta G$  titanium oxide = -759 kJ/mol,  $\Delta G$  nickel oxide = -147 kJ/mol) [8]. Hydroxylapatite is observed to be formed on the surface of the samples that produced after treated with H<sub>2</sub>O<sub>2</sub> and KOH then immersed in the higher strength simulated body fluid 5 SBF for 14 days as shown in the XRD pattern in Fig.7

It had been proposed that titania induces apatite formation on it's surface because the formation of Ti-OH functional groups. Thus many Ti-OH groups are formed on their surfaces, and the ionic activity product of the apatite in the surrounding fluid is increased by the increase of  $\sum\text{OH}^-$  ion concentration. Ti-OH groups can induce apatite nucleation, while the increased ionic activity product accelerates apatite nucleation [14,15,16].

As shown in Fig.8, the released of Ni ion content of the porous samples of various porosity ratios (15.9%, 20.3%, 26.3% and 32.5% respectively) in 0.9% NaCl without surface treatment as a function of time is higher than the safety line. Therefore, it is necessary to modify the surface of porous samples and reduce the Ni ion releasing. The safety line refers to the acceptable Ni ion content for human body with prolonging time and the slope of this line is a constant of 0.5  $\mu\text{g}/\text{cm}^2/\text{week}$  [17,18]. It is observed from Fig.8 that the amount of Ni ion release decreases with decreasing the porosity because the exposure surface to 0.9% NaCl of samples that have high porosity is greater than that of the low porosity.

The amount of Ni ion release from the uncoated and coated samples of various porosity ratios (15.9%, 20.3%, 26.3% and 32.5% respectively) in 0.9%NaCl are plotted against time in Figs.9-12. It is observed from these figures that the amount of Ni ion release from the coated samples are much lower than that of the uncoated NiTi alloy samples. These coatings create a physical and chemical barrier against Ni oxidation and modify the oxidation path ways of Ni so these coatings eliminate the Ni ion release into the immersion solution[19, 20].

It can be seen from Figs.9-12 and Fig.13 that the released Ni ion content of samples that coated with composite coatings of TiO<sub>2</sub> and HA curves intersect the safety line and some of the points are lower than the safety line. While the released Ni content of the samples

treated with  $\text{TiO}_2$  is slightly higher than the safety line as shown in Figs.9-12 and Fig. 14. This gives indication that single coat of  $\text{TiO}_2$  is insufficient to reduce the Ni ion release below the safety line. However the Ni ion released from samples that coated with  $\text{TiO}_2$  coating much lower than the bare samples and is closed to the safety line.

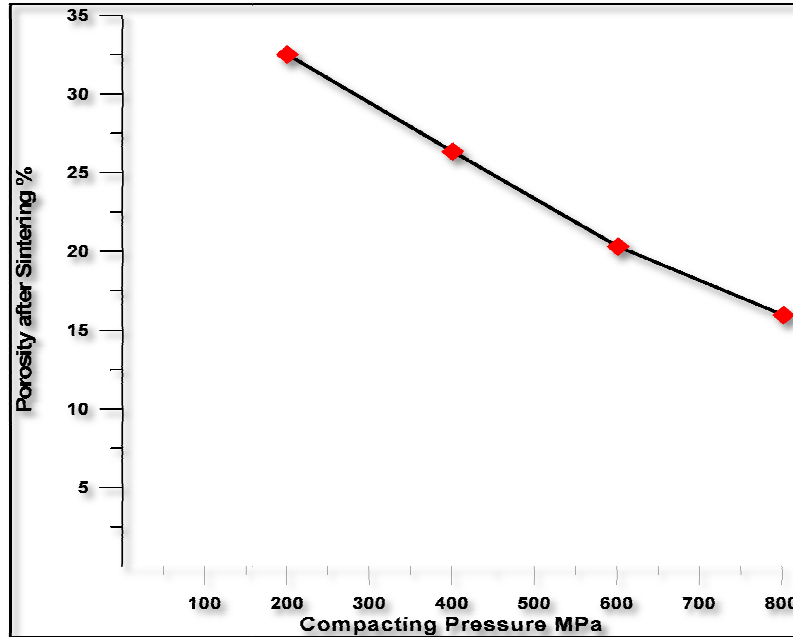


Fig.1 Green porosity as a function of compacting

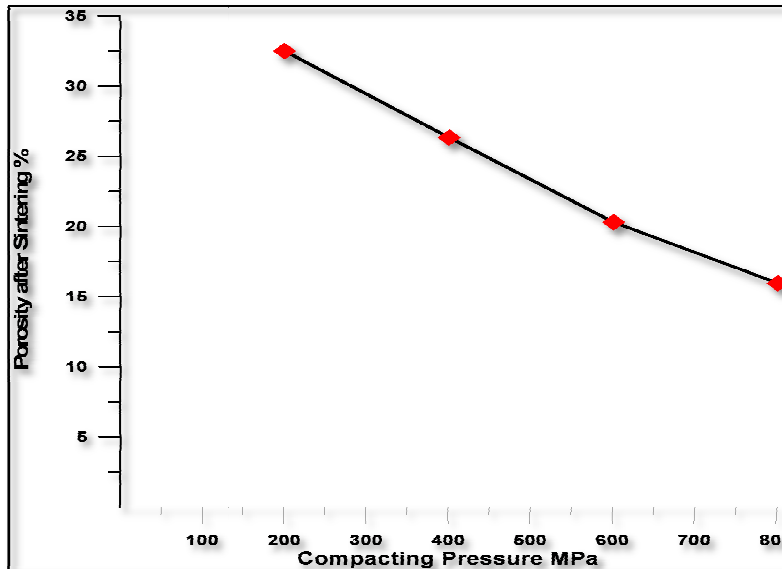


Fig. 2 Porosity after sintering as a function of compacting pressure.

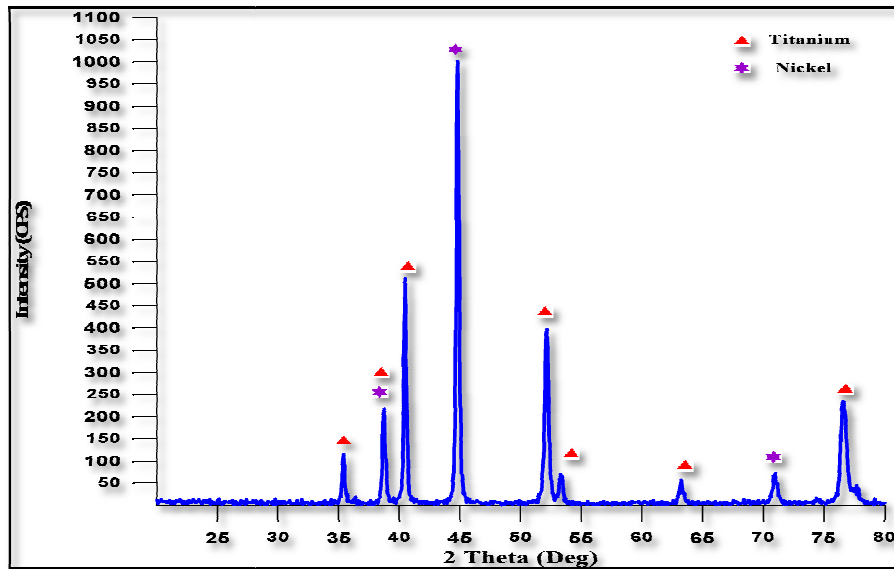


Fig.3 X-Ray diffraction for green compacted sample

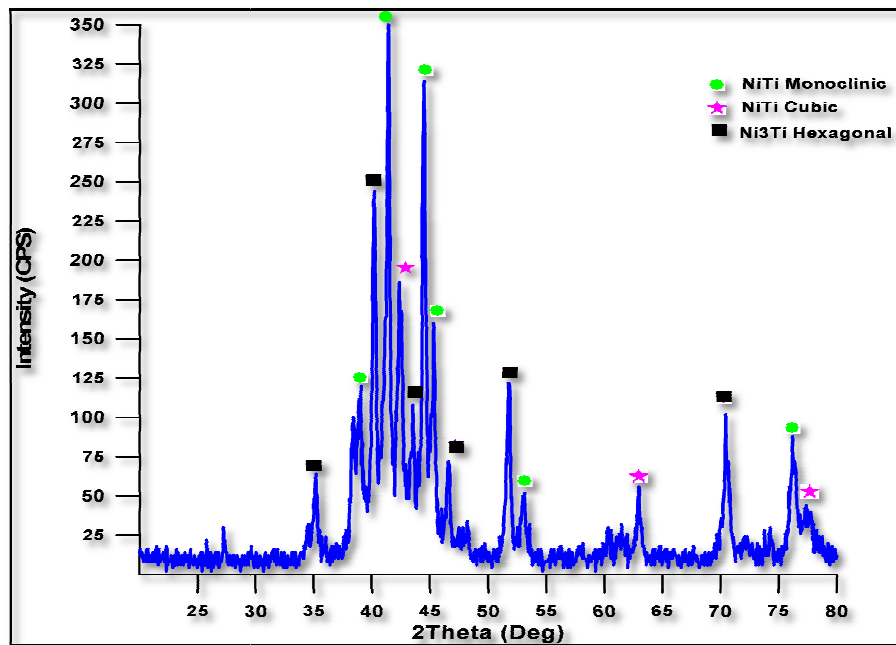


Fig.4 X-Ray diffraction after sintering at 975° C for 6 hours

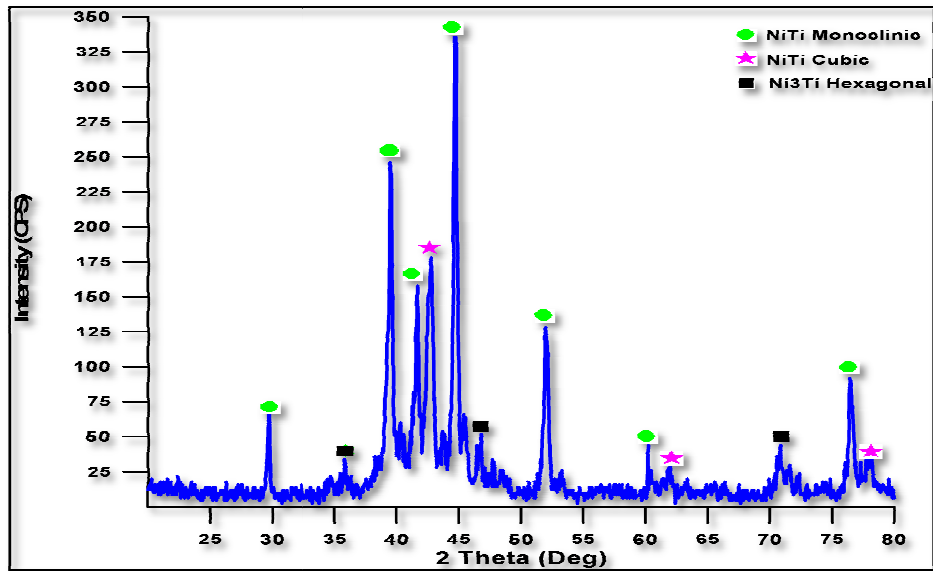


Fig.5 X-Ray diffraction after sintered at 975° C for 6 hours and then quenched from 900° C after soaking at 900° C for one hour in cold water.

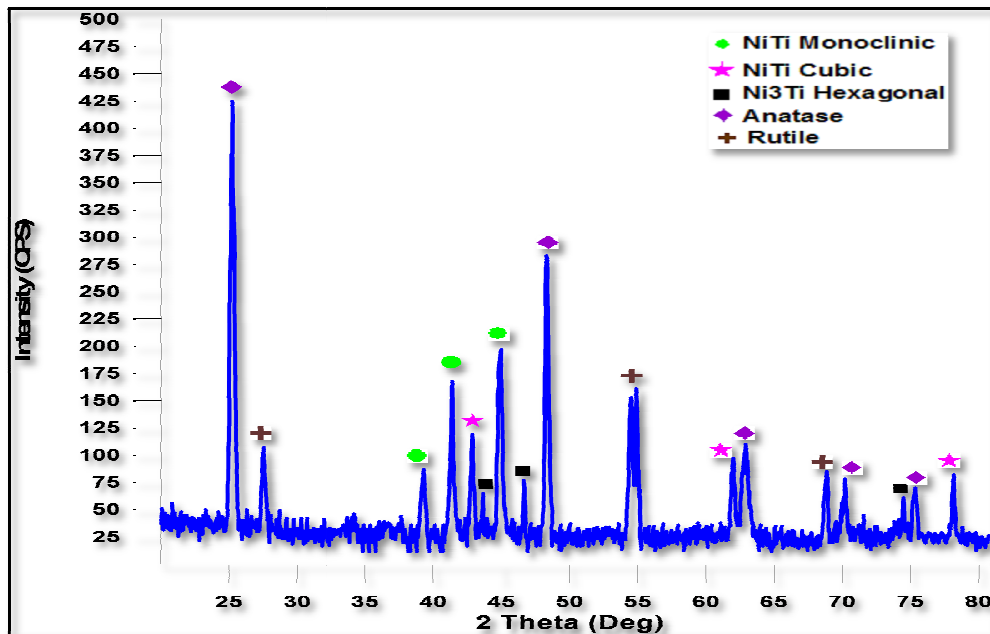


Fig. 6 X-Ray diffraction for samples treated with 35% $H_2O_2$  for two hours.



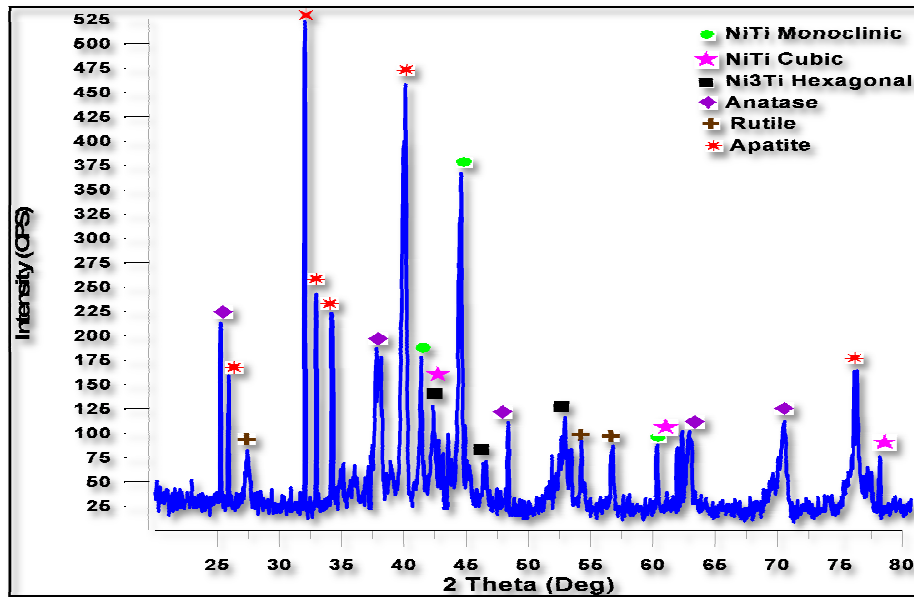


Fig. 7 X-Ray diffraction for samples treated with H<sub>2</sub>O<sub>2</sub> for two hours and KOH, then immersed in 5 SBF for 14 days .

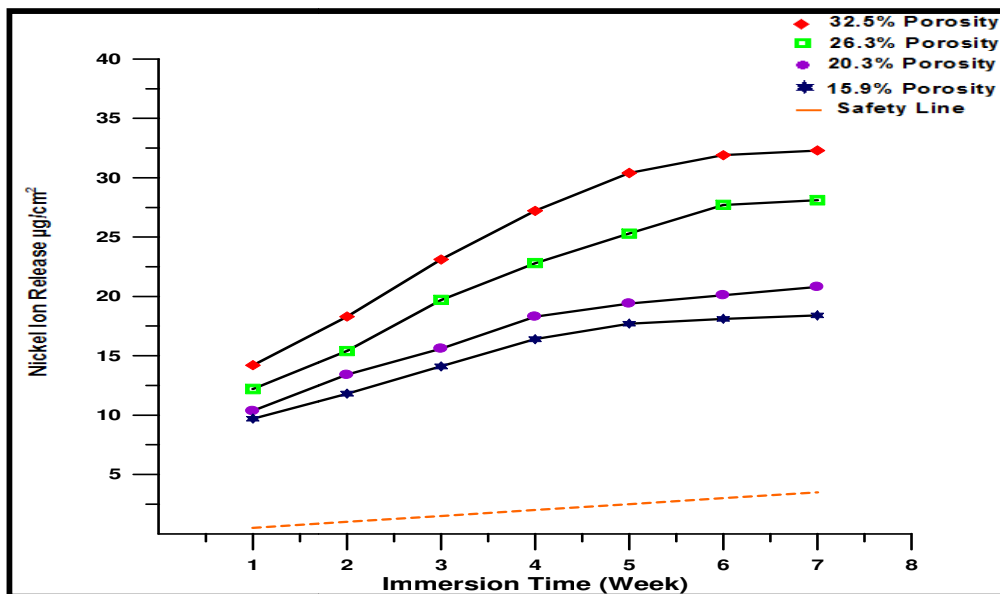


Fig. 8 Ni ion released in 0.9% NaCl against time for bare samples at various porosities.

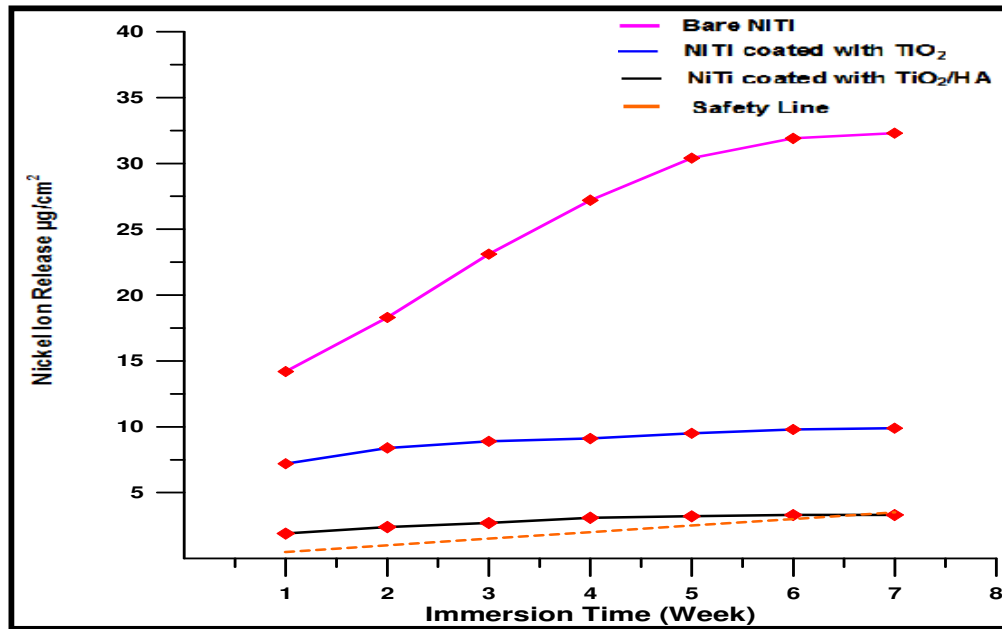


Fig. 9 Ni ion released in 0.9% NaCl against time for samples have 32.5% porosity.

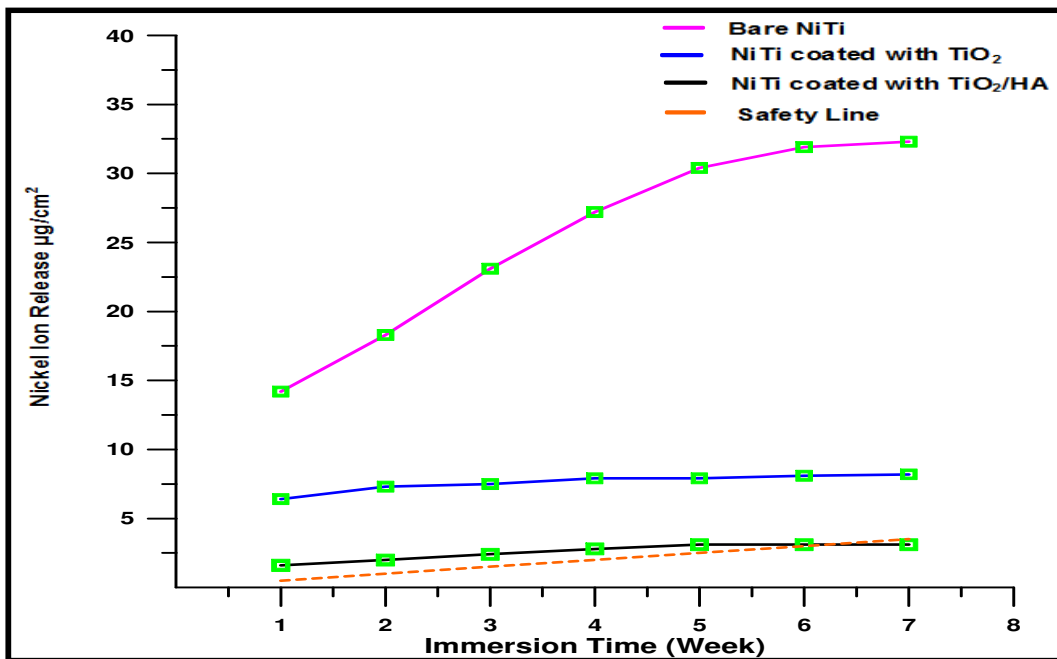


Fig. 10 Ni ion released in 0.9% NaCl against time for samples have 26.3% porosity.

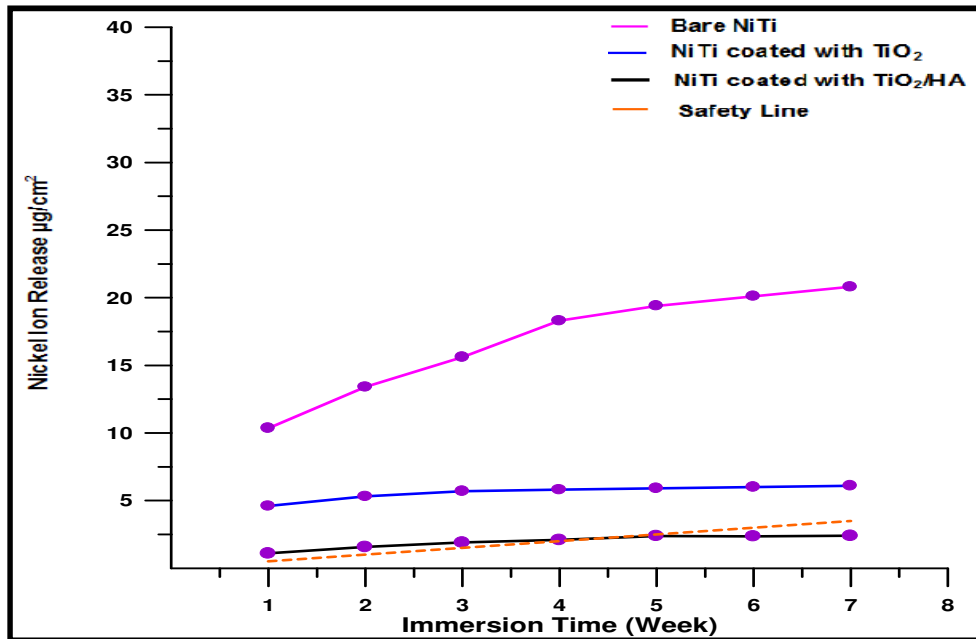


Fig. 11 Ni ion released in 0.9% NaCl against time for samples have 20.3% porosity.

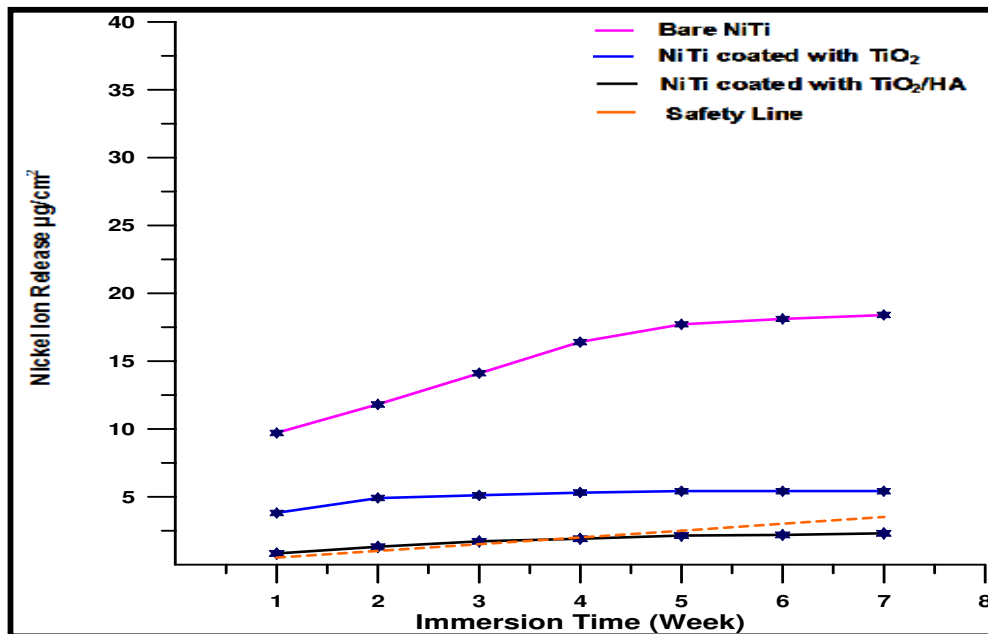


Fig. 12 Ni ion released in 0.9% NaCl against time for samples have 15.9% porosity.

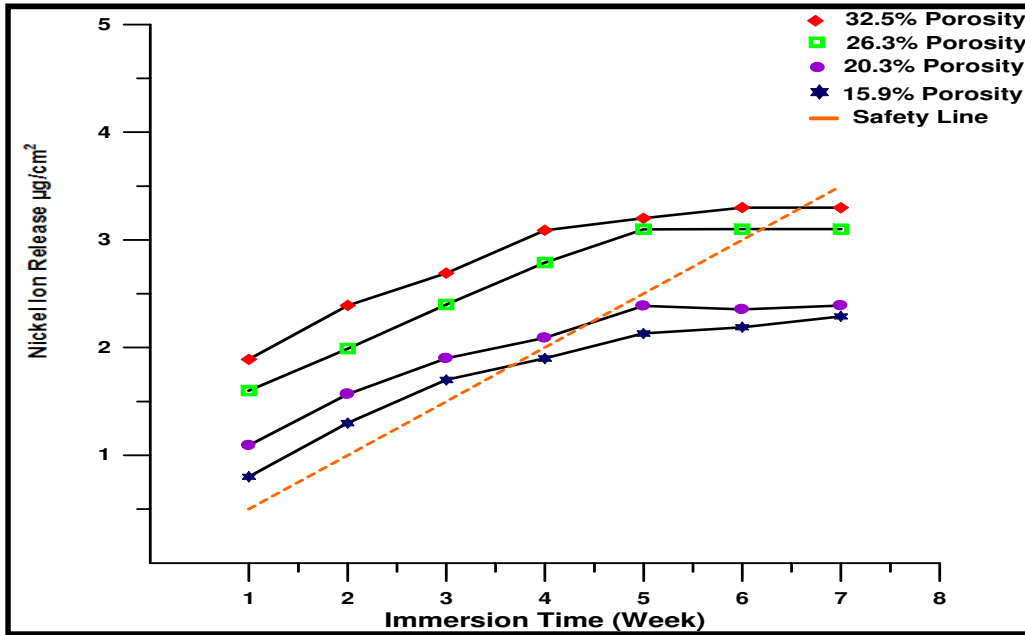


Fig. 13 Ni ion released in 0.9% NaCl against time for samples have composite coatings of TiO<sub>2</sub>/HA at different porosities.

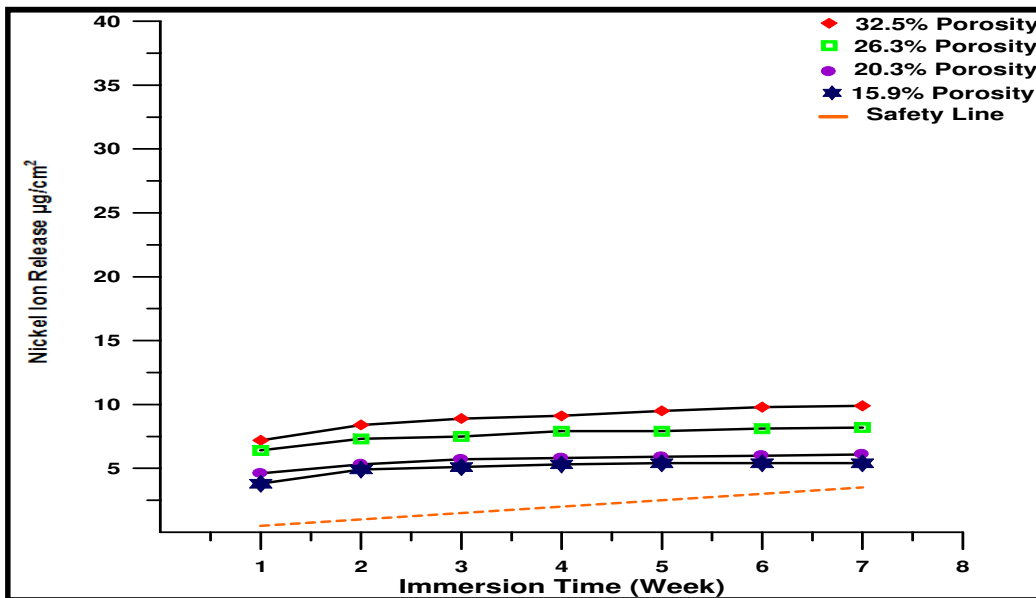


Fig. 14 Ni ion released in 0.9% NaCl against time for samples have TiO<sub>2</sub> coating at different porosities.

## **CONCLUSIONS**

- 1- Sintering at 975 °C for 6 hours with flowing of argon for equiatomic compacted powders of Ni and Ti result in complete sintering reaction and no pure metals were present.
- 2- Heat treatment porous NiTi shape memory alloys after sintering at 900°C for one hour with flowing of argon led reduce the amount of Ni<sub>3</sub>Ti phase.
- 3- The porosity of green compacted samples reduced after sintering process .
- 4- The Ni ion release increases with increasing porosity.
- 5- The porous NiTi is not safe to use in human body without surface treatment.
- 6- Ni ion released from coated porous NiTi SMA in 0.9% NaCl was decreased compared with bare NiTi SMA.
- 7- TiO<sub>2</sub>coating is insufficient to reduce the Ni release below the safety line, However the Ni ion released from samples that coated with TiO<sub>2</sub> coating much lower than the bare samples and close to the safety line.
- 8- Porous equiatomic NiTi SMA that coated with composite coatings TiO<sub>2</sub>/HA is save to use in human body because, the Ni ion released from samples that coated with composite coatings of TiO<sub>2</sub>/HA curves intersected the safety line and some of the points are lower than the safety line.

## **ACKNOWLEDGEMENTS**

The authors would like to acknowledge the University of Karbala in Iraqfor the provision of facilities.

- 1-Mel Schwartz" Encyclopedia of materials, parts, and finishes" Second Edition, CRC Press LLC, 2002.
- 2- T. Duerig , A. Pelton and D. Stoeckel "An overview of nitinol medical applications" Materials Science and Engineering A, Vols. 273-275,pp149 – 160, 1999.
- 3- X.T. Sun ,Z.X. Kang, X.L. Zhang, H.J. Jiang, R.F. Guana and X.P. Zhang "A comparative study on the corrosion behavior of porous and dense NiTi shape memory alloys in NaCl solution" Electrochimica Acta, Vol. 56, Issue18, pp. 6389– 6396 ,2011.
- 4- M.M. Verdian "Characterization and corrosion behavior of NiTi-Ti<sub>2</sub>Ni-Ni<sub>3</sub>Ti multiphase intermetallics produced by vacuum sintering" Journal of Vacuum, Vol.86, Issue 1, pp. 91-95,2011.
- 5- FU Tao, WU Xiao-ming, WU Feng , LUO Meng, DONG Bing-hui, and JI Yuan "Surface modification of NiTi alloy by sol-gel derived porous TiO<sub>2</sub> film" Trans. Nonferrous Met. Soc. China, Vol. 22, pp. 1661-1666, 2012 .
- 6 - Yong-Hua Li , Guang-Bin Rao , Li- JianRong and Yi-Yi Li "The influence of porosity on corrosion characteristics of porous NiTi alloy in simulated body fluid" Journal of Materials Letters, Issue 2, Vol. 57, pp. 448–451, 2002.
- 7- Yong-Hua Li, Guang-Bin Rao, Li-Jian Rong, Yi-Yi Li and Wei Ke "Effect of pores on corrosion characteristics of porous NiTi alloy in simulated body fluid" Journal of Materials Science and Engineering :A , Vol. 363, Issues 1-2, pp.356–359,2003.
- 8- Y.W. Gu, B.Y. Tay, C.S. Lim and M.S. Yong "Biomimetic deposition of apatite coating on surface-modified NiTi alloy" Journal of Biomaterials, Vol. 26, Issue 34, pp. 6916–6923 ,2005.

- 9-ASTM B-328 "Standard Test Method for Density, Oil Content, and Interconnected Porosity of Sintered Metal Structural Parts and Oil-Impregnated Bearings" ASTM International, 2003.
- 10- M.H. Wong , F.T. Cheng and H.C. Man "Characteristics, apatite-forming ability and corrosion resistance of NiTi surface modified by AC anodization" Journal of Applied Surface Science Vol. 255, Issue 18, pp.7527–7534,2007.
- 11-Emad Saadi AL-Hasani "Preparation and corrosion behavior of NiTi shape memory alloys " PhD thesis, Production Engineering and Metallurgy, University of Technology-Baghdad-Iraq, 2007.
- 12- S.L. Zhu, X.J. Yang , D.H. Fu, L.Y. Zhang c, C.Y Li c and Z.D. Cui "Stress–strain behavior of porous NiTi alloys prepared by powders sintering" Materials Science and Engineering A, Vol. 408, Issues 1–2, pp. 264–268, 2005.
- 13- ASM Materials Handbook "Alloy Phase Diagrams" Vol. 3, ASM International ,2005.
- 14- Mehrdad Keshmiri and Tom Troczynski "Apatite formation on TiO<sub>2</sub> anatase microspheres "Journal of Non-Crystalline Solids, Vol. 324, Issue 3, 2003.
- 15- Sirikul Wisutmethangoona and Nipon Denmud, Lek Sikong "Characteristics and compressive properties of porous NiTi alloys synthesized by SHS technique" Journal of Materials Science and Engineering A, Vol. 515, Issues 1-2, pp. 93–97, 2009.
- 16- Juan M. Ruso,Valeria Verdinelli,, Natalia Hassan, Olga Pieroni, and Paula V. Messina "Enhancing CaP biomimetic growth on TiO<sub>2</sub> cuboids nano particles via highly reactive facets" Journal of Langmuir, Vol. 29, Issue 7, pp. 2350–2358, 2013.
- 17- B. Yuan et al. H.Li ,Y.Gao , C.Y. Chung and M. Zhu "Passivation and oxygen ion implantation double surface treatment on porous NiTi shape memory alloys and its Ni suppression performance" Journal of Surface & Coatings Technology, Vol. 204, Issues 1-2,pp.58–63 ,2009.
- 18- B. Yuan M. Lai , Y. Gao , C.Y. Chung and M. Zhu "The effect of pore characteristics on Ni suppression of porous NiTi shape memory alloys modified by surface treatment" Journal of Thin Solid Films ,Vol.519 , Issue 13, pp.5297–5301, 2011.
- 19- Y. Cheng H. T. Li and Y. F. Zheng "Surface modification of NiTi alloy with tantalum to improve its biocompatibility and radiopacity " J Mater Sci , Vol.41, Issue 15, pp. 4961–4964,2006.
- 20- C.T. Kwok "Characterization and corrosion behavior of hydroxyapatite coatings on Ti6Al4V fabricated by electrophoretic deposition" J. Applied Surface Science, Vol. 255, Issues 13–14, pp. 6736–6744,2009.
- 21- Nilendu Krishna Paul and R.P.Nanda, "Shape Memory Alloy as Retrofitting Application in Historical Buildings and Monuments – A Review In Indian Perspective" International Journal of Civil Engineering & Technology (IJCIET), Volume 4, Issue 1, 2013, pp. 117 - 125, ISSN Print: 0976 – 6308, ISSN Online: 0976 – 6316.
- 22- N.Vijay Ponraj and Dr.G.Kalivarathan, "Densification and Deformation Behaviour of Sintered Powder Metallurgy Copper-7% Tungsten Composite During Cold Upsetting" International Journal of Mechanical Engineering & Technology (IJMET), Volume 4, Issue 1, 2013, pp. 1 - 7, ISSN Print: 0976 – 6340, ISSN Online: 0976 – 6359.